

Short Research Communication

Synthesis of Luminescent Near-Infrared AgInS₂ Nanocrystals as Optical Probes for In Vivo Applications

Liwei Liu¹, Rui Hu², Indrajit Roy³, Guimiao Lin², Ling Ye⁴, Jessica L. Reynolds⁵, Jianwei Liu⁴, Jing Liu⁴, Stanley A. Schwartz⁵, Xihe Zhang¹✉, and Ken-Tye Yong²✉

1. School of Science, Changchun University of Science and Technology, Changchun, 130022, P.R. China.
2. School of Electrical and Electronic Engineering, Nanyang Technological University, Singapore 639798, Singapore.
3. Department of Chemistry, University of Delhi, Delhi-110007, India.
4. Institute of Gerontology and Geriatrics, Laboratory Animal Center, Chinese PLA General Hospital, Beijing 100853, PR China.
5. Division of Allergy, Immunology and Rheumatology, Department of Medicine, State University of New York at Buffalo, Innovation Center, 640 Ellicott Street, Buffalo, NY 14203, USA.

✉ Corresponding author: Ken-Tye Yong, PhD, School of Electrical and Electronic Engineering, Nanyang Technological University, Singapore 639798, Singapore. Email: ktyong@ntu.edu.sg; Xihe Zhang, PhD, School of Science, Changchun University of Science and Technology, Changchun, 130022, P.R. China. Email: zhangxihe@cust.edu.cn.

© Ivyspring International Publisher. This is an open-access article distributed under the terms of the Creative Commons License (<http://creativecommons.org/licenses/by-nc-nd/3.0/>). Reproduction is permitted for personal, noncommercial use, provided that the article is in whole, unmodified, and properly cited.

Received: 2012.08.30; Accepted: 2012.10.15; Published: 2013.02.01

Abstract

Near infrared quantum dots have been receiving great attention as fluorescent optical probes for in vivo imaging applications. In this contribution, we report the synthesis and surface functionalization of cadmium free ternary AgInS₂ nanocrystals emitting in the near infrared range for successful in vitro and in vivo bioimaging applications. The FDA approved triblock copolymer Pluronic F127 was used to encapsulate the nanocrystals and made them dispersible in aqueous solution. By employing a whole body small animal optical imaging setup, we were able to use the AgInS₂ nanocrystals formulation for passive targeted delivery to the tumor site. The ultra-small crystal size, near-infrared emitting luminescence, and high quantum yield make the AgInS₂ nanocrystals an attractive candidate as a biological contrast agent for cancer sensing and imaging.

Key words: Near infrared quantum dots, Bioimaging, Surface functionalization, Targeted delivery, Nanotoxicity.

INTRODUCTION

Semiconductor nanocrystals (NCs), also known as quantum dots (QDs), are of great interest for applications ranging from biomedical imaging to biosensing[1-8]. CdSe and CdTe nanocrystals have been intensively used as probes in biological applications for the past few years[9-14]. However, the potential toxicity of cadmium from these nanocrystals remains a major roadblock for future applicability of these NCs in clinical trials, particularly in view of environmental and health regulations[15-19]. To overcome these challenges, two general strategies are proposed, which are either modifying the NC surface

with long lasting biocompatible polymers to prevent the degradation of the NCs or engineering cadmium-free NCs[20-23]. In view of this objective, some research groups are currently focusing on the fabrication of cadmium-free NCs for biological applications[24].

Ternary I-III-VI semiconductor NCs offer an interesting alternative for bioimaging applications[25]. AgInS₂ is a direct band gap semiconductor and belongs to the I-III-VI bulk crystals family with a band gap of ~1.8 eV at room temperature[26, 27]. This indicates that it is possible to engi-

near AgInS₂ nanocrystal that emits in the near-infrared range with high extinction coefficients, which is optimal for imaging deep-sitting tumors. More importantly, AgInS₂ NCs are more acceptable for real-world biological applications because AgInS₂ NC does not contain any cadmium, lead, mercury, selenium, tellurium, and arsenide, upon comparing to currently used NCs in biomedical applications. Thus, AgInS₂ NCs are promising candidates for efficient *in vitro* and *in vivo* imaging and sensing. Although in the most recent reports AgInS₂ system with quantum yield (QY) up to 30% have been shown[28], this value is lower than those of II–VI semiconductor core/shell NCs, with QY as high as 85%. Nevertheless, the QY obtained from the AgInS₂ NCs ternary system is sufficient for *in vivo* imaging applications, especially for the NCs that emits in the near-infrared range as they have high signal-to-noise ratio.

This work reports the controlled synthesis of functionalized AgInS₂ NCs as biological probes for tumor targeting and imaging in live animals. More specifically, we demonstrated a straightforward synthesis approach in fabricating water-dispersible near-infrared AgInS₂ NCs with QY as high as 35%. In our approach, AgInS₂ NCs were first prepared using the hot colloidal synthesis method. The resulting NCs were subsequently encapsulated within the Pluronic F127 triblock copolymer micelle for rendering them dispersible in biological buffers. These encapsulated particles were then used as biological luminescent probes for *in vitro* and *in vivo* tumor targeted imaging. Our studies have demonstrated that the micelle-encapsulated NC formulation was able to target the tumor site following tail vein injection of the NCs into the small animals. The biotoxicity of micelle-encapsulated AgInS₂ NCs was evaluated by using a whole-body small animal optical imaging system, together with tissues section analysis, and small animal behavior evaluation.

MATERIALS AND EXPERIMENTAL METHODS

Synthesis of AgInS₂ NCs

An oleylamine-sulfur solution was prepared by dissolving 0.1926 g of sulfur (6 mmol) in 5 mL of oleylamine. Separately, 1 mmol of indium acetate, 1 mmol of silver nitrate, 2 mL of oleic acid, 3 mmol of stearic acid were dissolved in 15 mL of octadecene. The mixture solution was heated at 85°C for 45 minutes under argon flow, then 10 mmol of dodecanethiol and 3 mL oleylamine-sulfur solution were injected under vigorous stirring into the hot reaction mixture. The reaction mixture was held at 120°C and

stirred for ~15 minutes and then an aliquot was removed by syringe and injected into a large volume of toluene at room temperature to quench the reaction. The NCs were separated from the chloroform solution by the addition of ethanol and followed by centrifugation. The NC precipitate could be redispersed in various organic solvents including hexane, toluene, and chloroform.

Preparation of copolymer-micelle coated NCs

The as-prepared organic-dispersible NCs were separated from the surfactant solution by addition of ethanol followed by centrifugation at 12000 rpm for 20 minutes. The precipitate was collected and dried in vacuum and re-dispersed in chloroform. Next, the NC stock chloroform solution (~3 mg/mL), and triblock copolymer (Pluronic F127) chloroform solution (~20 mg/mL) were mixed together at a volume ratio of 1:1. A vacuum Buchi rotary evaporator with a water bath at room temperature was used to evaporate the organic solvent. The lipidic film, deposited on the round bottom reaction flask, was hydrated with 1 mL of HPLC water and subjected to ultrasonication for 20 minutes using a bath sonicator. To remove the excess copolymer from the NC dispersion, the micelle-encapsulated NCs were further purified using centrifugation at 10000 rpm for 15 minutes.

Characterization of AgInS₂ nanocrystals structure

High Resolution Transmission Electron Microscopy images of as prepared nanocrystals were obtained using a JEOL model JEM 2010 microscope at an acceleration voltage of 200 kV. Powder X-ray diffraction (XRD) patterns were recorded using a Siemens D500 diffractometer, with Cu K α radiation.

Optical properties characterization of AgInS₂ NCs

The absorption spectra of NCs were collected using a Shimadzu model UV-2450 spectrophotometer over the wavelength range from 450 to 900 nm. The samples were measured against chloroform or water as reference. The NC emission spectra were collected using a Fluorolog-3 Spectrofluorometer (Edison, NJ USA). The excitation wavelength was set at 450 nm and the emission scanned from 500 to 1300 nm. Fluorescence quantum yields (QYs) of the NC dispersions were estimated by comparing the integrated emission from the nanocrystals to rhodamine 6G dye solutions of matched absorbance. Samples were diluted so that they were optically thin. It should be noted that the measurement result of QY does not provide an absolute value yet rather an estimation for guidance ref-

erence. Fluorescence intensity decay measurements were performed using an EasyLife LS fluorescence lifetime system. A 650 nm excitation source was used in this study.

Particle Size Analysis

Dynamic light scattering (DLS) was used to study the NC hydrodynamic sizes. The DLS experiments were performed using the Brookhaven Instruments 90Plus particle size analyzer. All measurements were carried out at 25°C.

Evaluation of in vitro cytotoxicity

For each MTS assay, 24 culture wells of Panc-1 cells were prepared. Seven sets were treated with different concentration of NCs and one set was used as the control. The complete assay was performed thrice, and results were averaged. Various concentrations of Pluronic F127 encapsulated NCs formulation ranging from 50 to 500 µg/mL were added to each well and subsequently incubated with cells for 24 or 48 hours at 37 °C under 5% CO₂.

In vitro imaging studies

Blood donors were recruited at the University at Buffalo; consents were obtained consistent with the policies of University at Buffalo Health Sciences Institutional Review Board (HSIRB) and the National Institutes of Health. Peripheral blood samples from healthy individuals were drawn into a syringe containing heparin (20 units/ml, Sigma-Aldrich, St. Louis, MO). For the isolation of human peripheral blood monocyte-derived macrophages (MDM), peripheral blood mononuclear cells (PBMC) were separated by Ficoll-Paque (GE Health Care, Piscataway, NJ) gradient centrifugation. CD14⁺ cells were isolated from PBMC by direct positive isolation using Dynabeads CD14 (Invitrogen, Carlsbad, CA) according to the manufacturer's instructions. CD14⁺ cells were cultured in complete medium [RPMI 1640, 10% fetal calf serum, 5% human AB serum, 10 mM/L HEPES, 1% Penicillin-Streptomycin, 10 ng/ml macrophage colony-stimulating factor (Millipore, Billerica, MA)] for 7 days for differentiation into MDM. Cells (1x10⁵cells/ml) were the cultured on Lab-Tek chambered coverglasses (Nalgene Nunc International, Rochester, NY). The MDM were treated with Pluronic F127 encapsulated AgInS₂ NCs and imaged with Leica Tcs sp2 confocal imaging system. DAPI was used for the cell nuclear staining.

Small animal imaging studies

Radiation induced fibrosarcoma (RIF) cells were used to develop tumor xenografts in mice. Five weeks old nude female mice were purchased from experi-

mental animal center of Jilin university. The animal housing area was maintained at 24°C with a 12 hours light/dark cycle, and the animals were fed *ad libitum* with water and standard laboratory chow. The tumor cells were implanted subcutaneously on the mice shoulder. After the tumor grew to a suitable size, the mice were administered ~3 mg of NCs formulation in 1x PBS by tail vein injection. The mice treated with NCs were anesthetized for imaging using the Kodak Fx-Pro in vivo imaging system (Kodak, USA) and the images were obtained using the fluorochrome un-mixing technique in the vendor software.

RESULTS AND DISCUSSION

Figure 1 summarizes the physical and optical properties of the synthesized AgInS₂ NCs. The absorption spectra of the AgInS₂ NCs dispersions (both chloroform and aqueous) are shown in Figure 1a. From our measurements, they did not show any well-defined exciton absorption peaks, which is consistent with current literature reports. There are two reasons for the featureless absorption spectra in the ternary system NCs. The first is due to the special electronic properties of I-III-VI semiconductor NCs in comparison to II-VI semiconductor NCs. The second reason may be due to the variations in the composition of silver, indium and sulfur in AgInS₂ NC from particle to particle that affect the overall quantum confinement effects on the NCs. In our case, we speculate that the second reason might be the main factor contributes to the featureless absorption spectra. Figure 1b shows the photoluminescence spectra of AgInS₂ NCs excited at 660 nm. From this figure, one can observe that the normalized emission spectral curves are nearly identical for both NCs chloroform and aqueous dispersions with the emission peaks located around 800 nm and having a spectral bandwidth of 180 nm. The other important information that one can extract from Figure 1b is that the solvent effect on the emission spectra of the AgInS₂ NCs is insignificant. This suggests that the water dispersible AgInS₂ NCs is optically stable and can be employed for in vitro and in vivo cancer diagnosis and therapy. In addition to UV-Vis and photoluminescence measurements, we have also investigated the emission life-time of the AgInS₂ NCs sample. Figure 1c shows the measured normalized decay for the AgInS₂ solution, which we found could be well fitted by a double-exponential formula. Based on the fitting data, we can see that for the measured sample, there is a fast decay component with a decay constant of 110 ns and a slow decay component with a decay constant of 870 ns. This finding suggests that the AgInS₂ NCs have great potentials as real time and long-term imaging

contrast agents in comparison with the cadmium-based NCs.

Figure 1d shows the TEM image of organically dispersible AgInS₂ NCs. It revealed that the crystals were generally in a spherical shape, mixed with some slightly elongated shapes. The size of the nanocrystals is estimated to be 3.5–4.5 nm. The TEM image of these NCs following their aqueous dispersion via encapsulation within Pluronic F127 block copolymer micelles is shown in Figure 1e. A comparison between Figure 1d and 1e shows that the size of the NCs remains unchanged before and after encapsulation within the block copolymer micelles. Figure 1f is the powder X-ray diffraction (XRD) profile for the AgInS₂ NCs. The XRD pattern of the AgInS₂ NCs matches well with the tetragonal structure of bulk AgInS₂ crystals that show the major diffraction peaks at (112), (204), and (312) planes. Also, the composition of AgInS₂ NCs was evaluated using energy-dispersive X-ray spectroscopy (EDS) analysis. The EDS analysis confirmed the composition of silver, indium, and sulfur with weight fractions of 39.06%, 35.82% and 25.12%, respectively. Dynamic light scattering was also used to determine the hydrodynamic size of the NCs formulation. The hydrodynamic size was estimated to be around 10 nm.

The cytotoxicity of micelle-encapsulated AgInS₂ NCs was also investigated. It is important to prepare biocompatible NCs for them to be realized in applications ranging from *in vitro* to *in vivo* imaging. The cytotoxicity of cadmium-based NCs has been well studied previously. However, there exists no systematic research of cytotoxicity of AgInS₂ NCs. With these motivations, in this study, we have assessed the cytotoxicity of the AgInS₂ NC sample on human pancreatic cancer cells (Panc-1) using the MTS assay. The relative viability of Panc-1 cells treated with NC formulation was determined after 24 and 48 hours exposure as presented in Figure 2. Exposure of the Panc-1 cells to micelle-encapsulated NCs led to a very small change in cell viability. Figure 2 shows that cells treated with micelle-encapsulated NCs for both 24 and 48 hours maintained greater than 80% cell viability even at NCs concentration as high as 500 µg/mL, suggesting minimal cytotoxicity associated with these QDs. Also, we demonstrated here the *in vitro* fluorescent labeling capability of these aqueous dispersive NCs. The inset of Figure 2 clearly shows the uptake of the Pluronic F127 encapsulated AgInS₂ NCs in red by human peripheral blood monocyte-derived macrophages (MDMs).

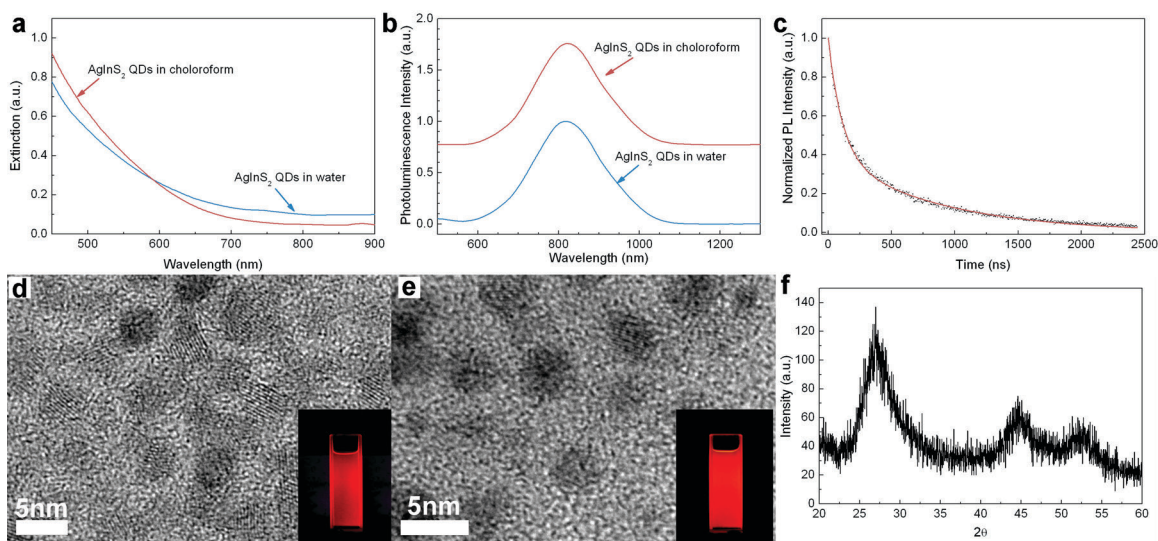


Figure 1. Absorption (a) and photoluminescence (b) spectrum of AgInS₂ nanocrystals (NCs) dispersed in either chloroform (as synthesized) or water (after Pluronic F127 micelle-encapsulation). (c) Fluorescence decay (dotted) of NCs chloroform solution sample and the best double-exponential fitting curve (red line). (d) and (e) are TEM images of AgInS₂ NCs dispersed in chloroform and water, respectively. Two insets are pictures taken under UV light excitation. (f) The XRD profile of AgInS₂ NCs.

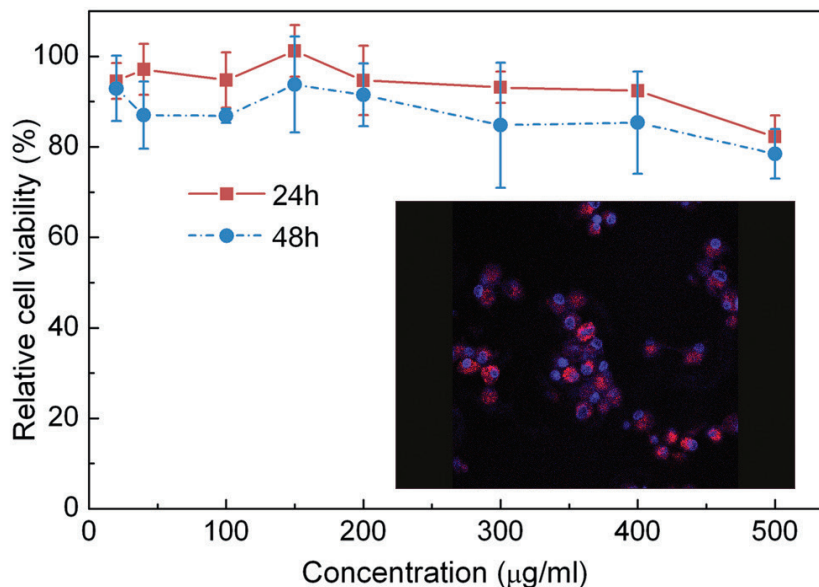


Figure 2. Relative viability of Panc-1 cells at 24 (square) and 48 hours (circle) of post-treatment in the presence of micelle-encapsulated AgInS₂ NCs. Inset is a confocal fluorescent image of macrophages treated with Pluronic F127 encapsulated AgInS₂ NCs. Red signals are from the AgInS₂ NCs and blue signals are from DAPI stained cell nucleus.

To test the ability of the micelle-encapsulated NCs as optical probes for *in vivo* tumor imaging, we performed small animal whole body near-infrared luminescence imaging on NCs treated tumor-bearing mice, where the AgInS₂ NCs formulation was intravenously administered into the mice. Figure 3 shows the spectral unmixed *in vivo* luminescence images of a tumor-bearing mouse treated with the micelle-encapsulated NCs, where the signals from AgInS₂ NCs are pseudo-colored in red and the background fluorescence in violet. We have found that the micelle-encapsulated NCs accumulated in tumor as early as 15 minutes post-injection. The subcutaneous tumor can be easily distinguished from the background tissue, demonstrating the excellent tumor targeting ability of micelle-encapsulated NCs. For the next 24 hours, the NCs luminescence intensity in the tumor gradually decreased. This excellent tumor targeting ability of micelle-encapsulated NCs might be suitable for the drug delivery of cancer therapy because anticancer drug-loaded NCs can release highly concentrated anticancer drugs into tumors for a long time. In our *in vivo* study, the functionalized NCs accumulated in the tumor site through passive targeting, which is a commonly used therapeutic approach for cancer therapy by accumulating NC particles in tumor tissue through the enhanced permeability and retention (EPR) effect[29]. Tumor tissue accumulation is a passive process that requires a long

circulating half-life to facilitate time-dependent extravasations of nanoparticles delivery systems through the leaky tumor microvasculature and accumulated in the tumor tissue. This process is dependent on the biophysicochemical properties of the NCs formulation. Therefore, even in the absence of targeting biomolecules such as antibodies, micelle-encapsulated NCs can still be used to target the tumor tissue. Recently, we have reported the biodistribution study of micelle-encapsulated QDs using nonhuman primate model[14]. The results have shown that majority of the QDs was removed from the blood circulation after 1 hour and accumulated in the liver and spleen as time progressed. It's worth noting that the functionalized AgInS₂ NCs formulation in this study is speculated to have similar biodistribution trend since it shares almost the same surface coating as well as the hydrodynamic diameter with the QDs formulation used in the monkey study. As a result, the AgInS₂ NCs are most likely gathered in the liver and spleen 80 minutes post-injection and this consequently causes a significant drop in the fluorescent intensity from the tumor as shown in Figure 3.

In this study, we performed histological analysis of acute toxicity induced by intravenous administration of NCs on the major organs, such as liver, lung, spleen, kidney, brain and heart of mice. As shown in Figure 4, small animals treated with Pluronic micelle-encapsulated AgInS₂ NCs did not show any

tissue injury on the liver, kidney, lung, and heart, demonstrating the low toxicity of the formulation. Also, body weight changes have been employed to examine the acute toxicity of small animals. No significant difference in body weight was observed be-

tween NCs treated and control mice for more than 1 week. More importantly, we have found that no changes in eating, drinking, or activity in the mice treated with approximately 100 mg/kg of the functionalized NC formulation.

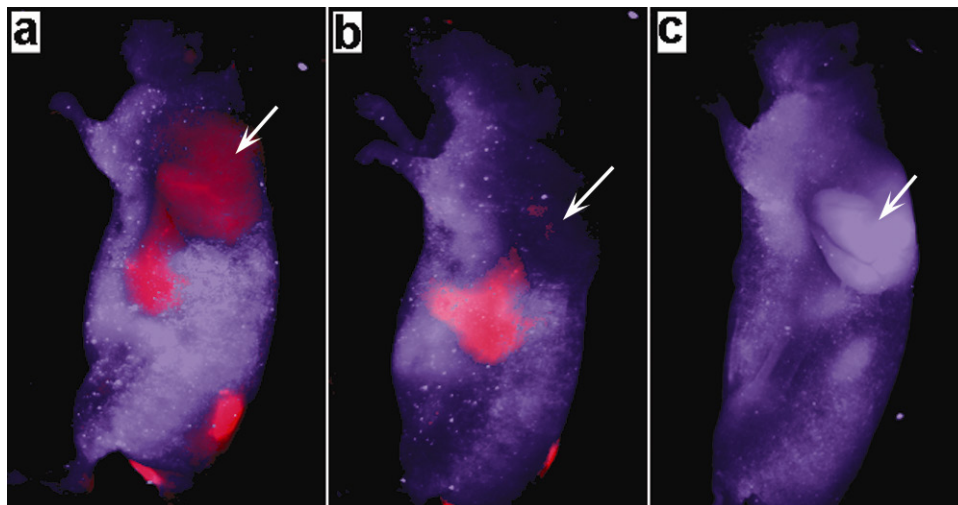


Figure 3. Time dependent in vivo luminescence imaging of tumor-bearing mice (tumor pointed by white arrows) injected with 3 mg of triblock copolymer micelle-coated NIR NCs. All images were acquired under the same experimental conditions. (a) 15 min; (b) 80 min; and (c) 24 hrs post-injection. The autofluorescence from tumor-bearing mice is shown in violet and the unmixed near-infrared NC signal is coded in red.

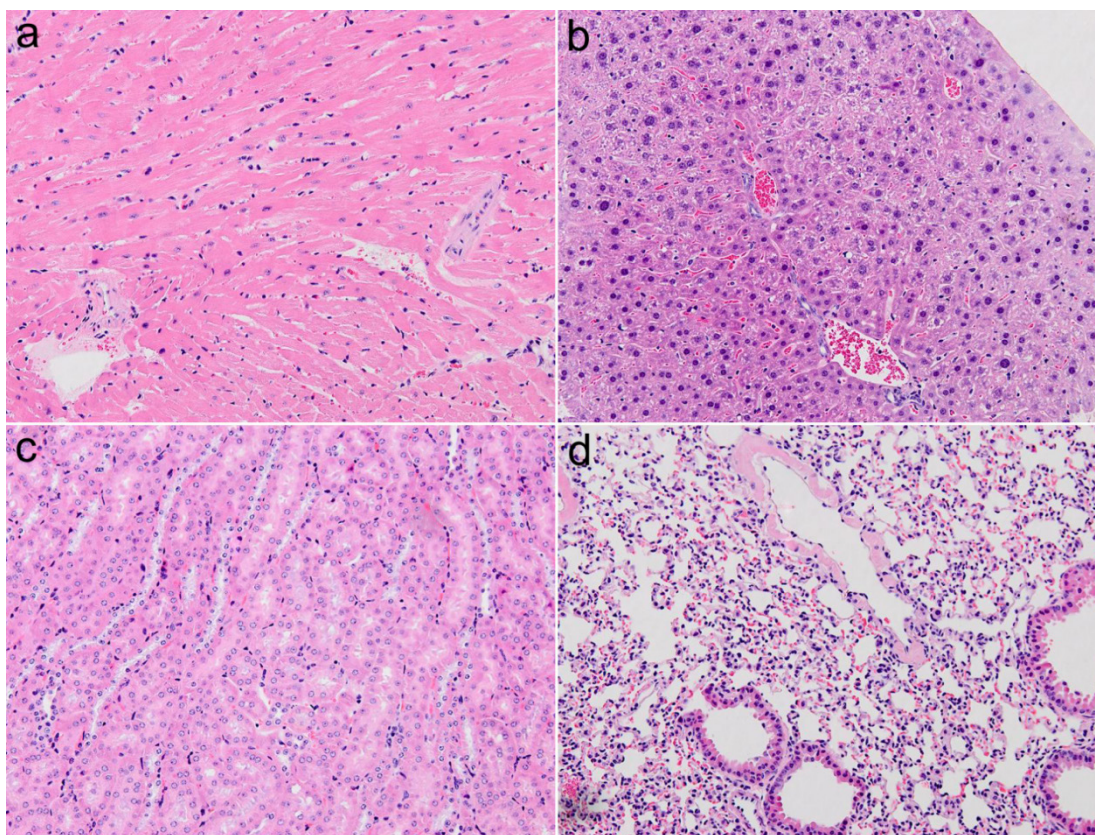


Figure 4. H&E-stained tissue sections from a SKH-I nude mouse administered with micelle-encapsulated AgInS₂ NCs 1 week post injection. Tissues were harvested from heart (a), liver (b), kidney (c), and lung (d), respectively.

CONCLUSION

In conclusion, we have successfully fabricated water-dispersible highly luminescent AgInS₂ NCs as near-infrared probes for targeting and imaging of tumors in vivo. The resulting micelle-encapsulated NCs formulation exhibited sharp PL spectra and the emission can be made to be at in the near-infrared range with QY as high as 35%. By employing a whole body small animal optical imaging setup, we were able to use the AgInS₂ NCs formulation for passive targeted delivery to the tumor site. The ultra-small crystal size, near-infrared emitting luminescence, and high QY make the AgInS₂ NCs an attractive candidate as a biological contrast agent for cancer sensing and imaging.

Acknowledgements

This work was supported by the Changchun University of Science and Technology, Singapore Ministry of Education (Grants Tier 2 MOE2010-T2-2-010 (M4020020.040 ARC2/11) and Tier 1 M4010360.040 RG29/10), Nanyang Technological University (start-up grant no. M4080141.040), the Beijing Natural Science Foundation (no. 7092097) and the National Natural Science Foundation of China (no. 21071150).

Competing Interests

The authors have declared that no competing interest exists.

References

- Alivisatos AP. Perspectives on the Physical Chemistry of Semiconductor Nanocrystals. *J Phys Chem.* 1996; 100: 13226-39.
- Chan WCW, Nie S. Quantum Dot Bioconjugates for Ultrasensitive Nonisotopic Detection. *Science.* 1998; 281: 2016-8. doi:10.1126/science.281.5385.2016.
- Chen B, Liu Q, Zhang Y, Xu L, Fang X. Transmembrane Delivery of the Cell-Penetrating Peptide Conjugated Semiconductor Quantum Dots. *Langmuir.* 2008; 24: 11866-71. doi:10.1021/la802048s.
- Gao X, Chen J, Chen J, Wu B, Chen H, Jiang X. Quantum Dots Bearing Lectin-Functionalized Nanoparticles as a Platform for In Vivo Brain Imaging. *Bioconjugate Chemistry.* 2008; 19: 2189-95. doi:10.1021/bc8002698.
- Kobayashi H, Hama Y, Koyama Y, Barrett T, Regino CAS, Urano Y, et al. Simultaneous Multicolor Imaging of Five Different Lymphatic Basins Using Quantum Dots. *Nano Letters.* 2007; 7: 1711-6. doi:10.1021/nl0707003.
- Kuo Y-C, Wang Q, Ruengruglikit C, Yu H, Huang Q. Antibody-Conjugated CdTe Quantum Dots for Escherichia coli Detection. *The Journal of Physical Chemistry C.* 2008; 112: 4818-24. doi:10.1021/jp076209h.
- Yezhelyev MV, Qi L, O'Regan RM, Nie S, Gao X. Proton-Sponge Coated Quantum Dots for siRNA Delivery and Intracellular Imaging. *Journal of the American Chemical Society.* 2008; 130: 9006-12. doi:10.1021/ja800086u.
- Yong K-T, Qian J, Roy I, Lee HH, Bergey EJ, Trampusch KM, et al. Quantum Rod Bioconjugates as Targeted Probes for Confocal and Two-Photon Fluorescence Imaging of Cancer Cells. *Nano Letters.* 2007; 7: 761-5. doi:10.1021/nl063031m.
- Bruchez M, Jr., Moronne M, Gin P, Weiss S, Alivisatos AP. Semiconductor Nanocrystals as Fluorescent Biological Labels. *Science.* 1998; 281: 2013-6. doi:10.1126/science.281.5385.2013.
- Gil PR, Parak WJ. Composite Nanoparticles Take Aim at Cancer. *ACS Nano.* 2008; 2: 2200-5. doi:10.1021/nn800716j.
- Hyun BR, Chen H, Rey DA, Wise FW, Batt CA. Near-Infrared Fluorescence Imaging with Water-Soluble Lead Salt Quantum Dots. *The Journal of Physical Chemistry B.* 2007; 111: 5726-30. doi:10.1021/jp068455j.
- Insin N, Tracy JB, Lee H, Zimmer JP, Westervelt RM, Bawendi MG. Incorporation of Iron Oxide Nanoparticles and Quantum Dots into Silica Microspheres. *ACS Nano.* 2008; 2: 197-202. doi:10.1021/nn700344x.
- Jiang W, Singhal A, Zheng J, Wang C, Chan WCW. Optimizing the Synthesis of Red- to Near-IR-Emitting CdS-Capped CdTeSe_{1-x} Alloyed Quantum Dots for Biomedical Imaging. *Chemistry of Materials.* 2006; 18: 4845-54. doi:10.1021/cm061311x.
- Ye L, Yong KT, Liu L, Roy I, Hu R, Zhu J, et al. A pilot study in non-human primates shows no adverse response to intravenous injection of quantum dots. *Nature Nanotechnology.* 2012; 7: 453-8.
- Cho SJ, Maysinger D, Jain M, Röder B, Hackbarth S, Winnik FM. Long-Term Exposure to CdTe Quantum Dots Causes Functional Impairments in Live Cells. *Langmuir.* 2007; 23: 1974-80. doi:10.1021/la060093j.
- Derfus AM, Chan WCW, Bhatia SN. Probing the Cytotoxicity of Semiconductor Quantum Dots. *Nano Letters.* 2003; 4: 11-8. doi:10.1021/nl0347334.
- Fitzpatrick JAJ, Andreko SK, Ernst LA, Waggoner AS, Ballou B, Bruchez MP. Long-term Persistence and Spectral Blue Shifting of Quantum Dots in Vivo. *Nano Letters.* 2009; 9: 2736-41. doi:10.1021/nl901534q.
- Peng ZA, Peng X. Formation of High-Quality CdTe, CdSe, and CdS Nanocrystals Using CdO as Precursor. *Journal of the American Chemical Society.* 2000; 123: 183-4. doi:10.1021/ja003633m.
- Zhang Y, So MK, Rao J. Protease-Modulated Cellular Uptake of Quantum Dots. *Nano Letters.* 2006; 6: 1988-92. doi:10.1021/nl0611586.
- Erogbogbo F, Yong K-T, Roy I, Xu G, Prasad PN, Swihart MT. Biocompatible Luminescent Silicon Quantum Dots for Imaging of Cancer Cells. *ACS Nano.* 2008; 2: 873-8. doi:10.1021/nn700319z.
- Kim S-W, Zimmer JP, Ohnishi S, Tracy JB, Frangioni JV, Bawendi MG. Engineering InAs_xP_{1-x}/InP/ZnSe III-V Alloyed Core/Shell Quantum Dots for the Near-Infrared. *Journal of the American Chemical Society.* 2005; 127: 10526-32. doi:10.1021/ja0434331.
- Wang S, Jarrett BR, Kauzlarich SM, Louie AY. Core/Shell Quantum Dots with High Relaxivity and Photoluminescence for Multimodality Imaging. *Journal of the American Chemical Society.* 2007; 129: 3848-56. doi:10.1021/ja065996d.
- Yong K-T, Hu R, Roy I, Ding H, Vathy LA, Bergey EJ, et al. Tumor Targeting and Imaging in Live Animals with Functionalized Semiconductor Quantum Rods. *ACS Applied Materials & Interfaces.* 2009; 1: 710-9. doi:10.1021/am8002318.
- Yong K-T, Roy I, Swihart MT, Prasad PN. Multifunctional nanoparticles as biocompatible targeted probes for human cancer diagnosis and therapy. *Journal of Materials Chemistry.* 2009; 19: 4655-72.
- Li L, Daou TJ, Texier I, Kim Chi TT, Liem NQ, Reiss P. Highly Luminescent CuInS₂/ZnS Core/Shell Nanocrystals: Cadmium-Free Quantum Dots for In Vivo Imaging. *Chemistry of Materials.* 2009; 21: 2422-9. doi:10.1021/cm900103b.
- Li X, Niu JZ, Shen H, Xu W, Wang H, Li LS. Shape controlled synthesis of tadpole-like and heliotrope seed-like AgInS₂ nanocrystals. *CrystEngComm.* 2010; 12: 4410-5.
- Ogawa T, Kuzuya T, Hamanaka Y, Sumiyama K. Synthesis of Ag-In binary sulfide nanoparticles-structural tuning and their photoluminescence properties. *Journal of Materials Chemistry.* 2010; 20: 2226-31.
- Torimoto T, Adachi T, Okazaki K-i, Sakuraoaka M, Shibayama T, Ohtani B, et al. Facile Synthesis of ZnS-AgInS₂ Solid Solution Nanoparticles for a Color-Adjustable Luminophore. *Journal of the American Chemical Society.* 2007; 129: 12388-9. doi:10.1021/ja0750470.
- Farokhzad OC, Langer R. Impact of Nanotechnology on Drug Delivery. *ACS Nano.* 2009; 3: 16-20. doi:10.1021/nn900002m.